SF2A 2011
G. Alecian, K. Belkacem, R. Samadi and D. Valls-Gabaud (eds)

PARTICLE TRANSPORT AT RELATIVISTIC SHOCKS

I. Plotnikov[1]

Abstract. Relativistic shocks structure studied in recent analytical works and large Particle-In-Cell (PIC) simulations reports the existence of strong self-generated magnetic fields at the proximity of the shock front. These fields are generated by plasma instabilities (e.g. Weibel instability) and are turbulent on plasma skin depth scale. In this proceeding we present the study of particle transport in microturbulent isotropic magnetic field $\delta\vec{B}$ in the presence of external mean field $\vec{B}_0$, assuming $\langle\delta B^2\rangle \gg B_0^2$. The expression of parallel ($D_\parallel$) and transverse ($D_\perp$) diffusion coefficients are found. We find that $D_\parallel$ evolves as the square of particle energy and $D_\perp$ saturates when particle reduced rigidity ρ is greater then $\delta B/B_0$. Application to relativistic shocks upstream and downstream regions shows that the acceleration by Fermi mechanism is possible only for the range of particle rigidities where $1 < \rho < \delta B/B_0$.

Keywords: Turbulence, magnetic fields, particle diffusion

1 Introduction

High energy radiation from astrophysical objects as hot-spots of Active Galactic Nuclei (AGN) and Gamma Ray Bursts (GRBs) is usually expained by accelerated charged particles at relativistic shocks. In the case of GRBs external shock front attains Lorentz factors up to several hundreds ($\Gamma_s \sim 100$), providing an unique source involving ultra-relativistic blastwaves. It is logically expected that relativistic effects play an essential role in shock physics. For example, strong magnetic fields $> 10^{-4}$G in preshocked region are inferred from observations, difficult to explain as the ISM or ambient field strength (Li & Waxman 2006), but seem to be produced by the shock itself.

As supported by PIC simulations (Sironi & Spitkovsky 2011) relativistic shocks produce strong self-generated magnetic fields mediated by Weibel (filamentation) instability. Typical variation scale of such fields corresponds to plasma skin depth ($\sim 10^5$ m in the ISM). Larmor radius of individual particles with relativistic thermal energy $\Gamma_S m_p c^2$ in the downstream region appears to be always larger than this scale. Particle acceleration should be possible as long as the external magnetisation remains low, and produce non-thermal particle distribution with power-law tail $s = -2.24$. There are, however, no evidence of acceleration up to Very High Energies in relativistic shocks. In order to investigate particle acceleration we study the effects of intense small-scale turbulence on particle transport, adopting test-particle approximation. In following sections we present a study of transport of charged particles in intense small-scale turbulence and apply the results to constrain diffusive acceleration mechanism at relativistic shocks.

2 Particle trajectories

We consider particles with Larmor radius R_L greater than the magnetic field coherence length l_c. As astrophysical environments are always magnetised we superpose an external constant field $\vec{B}_0$ along z direction on turbulent self-generated field $\delta\vec{B}$, isotropic. To illustrate in simpliest way the behaviour of particles in small-scale magnetic turbulence we consider three different cases: regular magnetic field alone $B_0\vec{e}_z$, purely turbulent field with coherence length l_c smaller then the particle Larmor radius R_L, and two fields together with $\delta B >> B_0$ and $R_L/l_c >> 1$. In Fig. 1 field structure (top pannel) and corresponding particle trajectories (bottom panel) are presented. Constant field $\vec{B}_0$ produces the well-known helical particle trajectory (left column). $\delta\vec{B}$ alone

[1] UJF-Grenoble 1/CNRS-INSU, Institut de Planétologie et d'Astrophysique de Grenoble (IPAG) UMR 5274, 38041 Grenoble, France

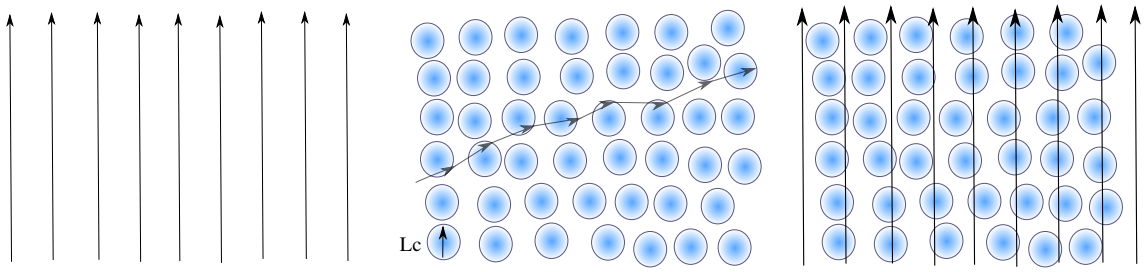

(a) Constant magnetic field along z. (b) Purely turbulent field with cohrence length l_c equal to the cell size. (c) Weak mean field superimposed on strong small-scale turbulence

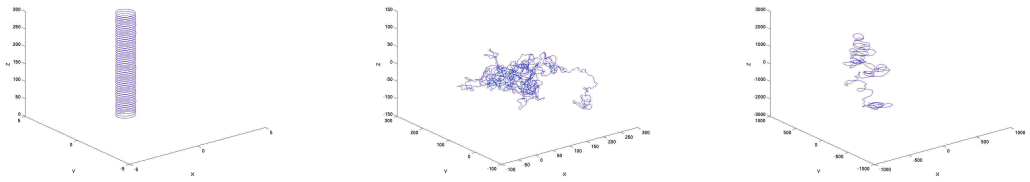

(d) Regular helical trajectory in constant magnetic field along z. (e) Random walk trajectory in purely turbulent field. (f) Weak mean field superimposed on strong small-scale turbulence (with $R_L \gg l_c$): perturbed helical trajectory.

Fig. 1: Example of three magnetic field structures (on the top panel) and corresponding particle trajectories (on the bottom pannel).

produces isotropic "random walk" trajectories (middle column). The superposed $\vec{B_0}$ and $\delta\vec{B}$ produce a moderately pertubed helical trajectory (right column). It is interesting to note that the trajectory is not isotropic despite that $\langle\delta B^2\rangle/B_0^2 >> 1$. It illustrates the effect of smallness of l_c compared to R_L. Hence, one cannot neglect the mean field, even very weak in comparison to $\delta\vec{B}$.

3 Transport in small-cale turbulence: theory and simulations

Only one physical assumption is necessary to deduce transport coefficients when $R_L >> l_c$: scattering time is greater than turbulent field coherence time $\tau_s >> \tau_c$. Consider random rotations from $\delta\vec{B}$ field and regular deflexion in (x, y) plane from $\vec{B_0}$ field. Then one may obtain diffusion coefficients expressions as (Plotnikov et al. 2011)

$$D_{\parallel} = \frac{c^2}{3\nu_s}, \qquad D_{\perp} = \frac{c^2}{3}\frac{\nu_s}{\omega_{L|0}^2+\nu_s^2}, \qquad \text{where} \nu_s = \frac{2c}{3\eta\rho^2}\ , \tag{3.1}$$

where the subscripts $\parallel$ ans $\perp$ signify respectively parallel and transverse to $\vec{B_0}$, ν_s is the angular scattering frequency, $\omega_{L|0}$ is the Larmor pulsation in B_0 field only ($\omega_{L|0} = qB_0/\gamma mc$), ρ is the particle reduced rigidity and $\eta = \langle\delta B^2\rangle/(\langle\delta B^2\rangle + B_0^2)$ is the field degree of turbulence.

When $\rho \gg 1$, $\omega_{L|0} >> \nu_s$, so as $D_{\perp} \simeq c^2/3\nu_s/\omega_{L|0}^2 = 2cl_c/9B_0^2 + \langle\delta B^2\rangle/B_0^2$. Hence it is independent of particle energy and governed by turbulence strength only.

Numerical Monte-Carlo simulations were performed in the same spirit as in Casse et al. (2002). Numerical scheme consists in integrating a large number of trajectories in random $\delta\vec{B}$ realization. Then statistical estimates of $D_{\parallel}$ and $D_{\perp}$ were obtained as the mean square of displacements from initial particle position divided by Δt. We expored the range of rigidities going from 1 to 10^2 and turbulence degree $\langle\delta B^2\rangle/B_0^2$ was varied between 1 and 10^4. Results are presented in Fig. 2 were parallel (left side) and perpendicular (right side) diffusion coefficient are plotted as function of numerical rigidity $\rho' = 2\pi R_L/L_{max}$, where $L_{max} \simeq 10l_c$. As expected, $D_{\parallel} \propto \rho'^2$ independently of turbulence level. For $\rho' < \sqrt{\langle\delta B^2\rangle/B_0^2}$, $D_{\perp} \propto \rho'^2$ until it reaches the plateau

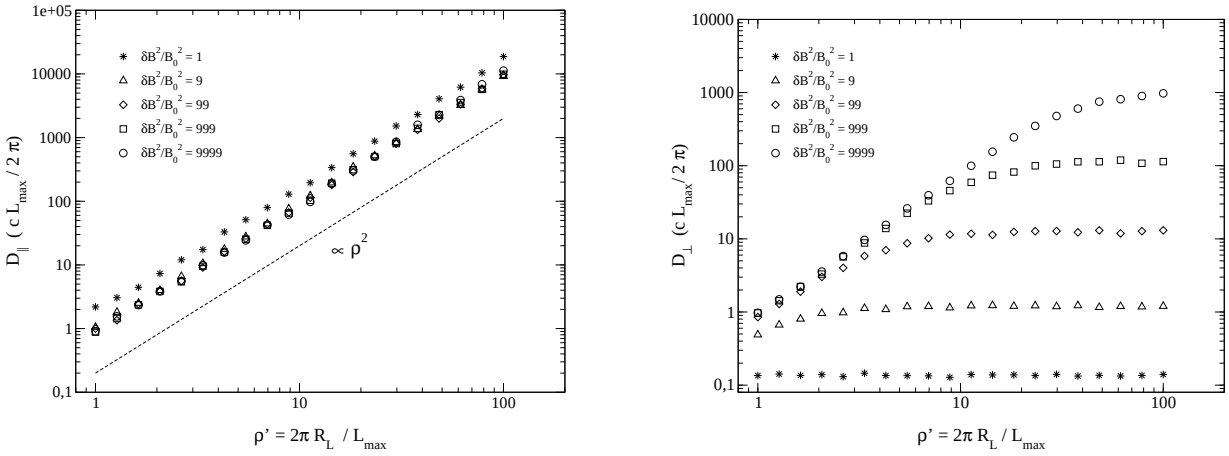

(a) $D_{\parallel}$ (b) $D_{\perp}$

Fig. 2: Diffusion coefficients $D_{\parallel}$(left panel) and $D_{\perp}$ (right panel) as function of reduced rigidity ρ'. The symbols correspond to various turbulence degrees $\langle \delta B^2 \rangle / B_0^2$ going from 1 to 10^4 as indicated. $D_{\parallel} \propto \rho'^2$ independently of turbulence level. For $\rho' < \sqrt{\langle \delta B^2 \rangle / B_0^2}$, $D_{\perp} \propto \rho'^2$ until it reaches the plateau at $\rho' \sim \sqrt{\langle \delta B^2 \rangle / B_0^2}$.

at $\rho' \sim \sqrt{\langle \delta B^2 \rangle / B_0^2}$. Both are in agreement with equations 3.1. Systematic presentation of the theory and simulations of this transport regime can be found in Plotnikov et al. (2011). At this point we can examine first-order Fermi acceleration mechanism when only small-scale turbulence is considered.

4 Application to upstream and downstream of relativistic shocks

The natural way to apply transport process is to concider two co-moving frames: upstream (unshocked medium, Laboratory frame) and downstream (shocked medium).

4.1 Upstream

In the upstream region the shock front move with the speed $V_{\rm s|u} \simeq c(1 - 1/\Gamma_S^2)$, very close to the lignt speed. Particles coming from downstream region are rapidly caught up by the shock front. The distribution function is consequently highly anisotropic, confined to the loss cone $\Delta\theta \simeq 2/\Gamma_S$ (Achterberg et al. 2001)

As argued in Lemoine et al. (2006) when only B_0 is present or when particles experiences large-scale turbulence with $\rho < 1$, acceleration process cannot take place due to field correletion between upstream and downstream region. If the field is turbulent on small scales ($R_{\rm L} > l_{\rm c}$) then the correlation disappears and diffusive acceleration is working. In the latter case, mean field deflective effect dominates over small-scale turbulence when ρ is large and returns are goverened mostly by B_0. The acceleration process may be quenched when $\rho >> 1$, as in the case of pure B_0 field. This is illustrated in Fig. 3 where phase space plots of entering (red dots) an escaping to downstream (blue dots) particles in three cases are plotted. Regular B_0 field deflects particles to the left (left panel, see also Achterberg et al. 2001). When small-scale turbulence is present and $\rho' \sim 1$ the distribution is isotropic in velocity space (middle panel) so that the acceleration is operative. With increasing energy $\rho' > \delta B/B_0$ and the turbulent field is no more able to isotropize the distribution. Particle residence time in the upstream region ($t_{\rm ups}$) is then : $\bar{t}_{\rm L}/\Gamma_S < t_{\rm ups} < t_{\rm L|0}/\Gamma_S$. Were $\bar{t}_{\rm L}$ and $t_{\rm L|0}$ are Larmor periods in the rms field and mean field alone, respectively. Lower limit applies when ρ is close to 1 and the upper limit applies when B_0 governs particle returns.

4.2 Downstream

Shock front speed in the downstream comoving frame is $V_{\rm s|d} \simeq c/3$. Shock compression of upstream magnetic field makes B_0 to be always perpendicular to the shock normal, therefore diffusive returns are governed by the transverse diffusion coefficient. Residence time is estimated as $t_{\rm dow} \simeq 18 D_{\perp}/c^2$. As result of $D_{\perp}$ saturation at highest energies, diffusive return time attains a finite value.

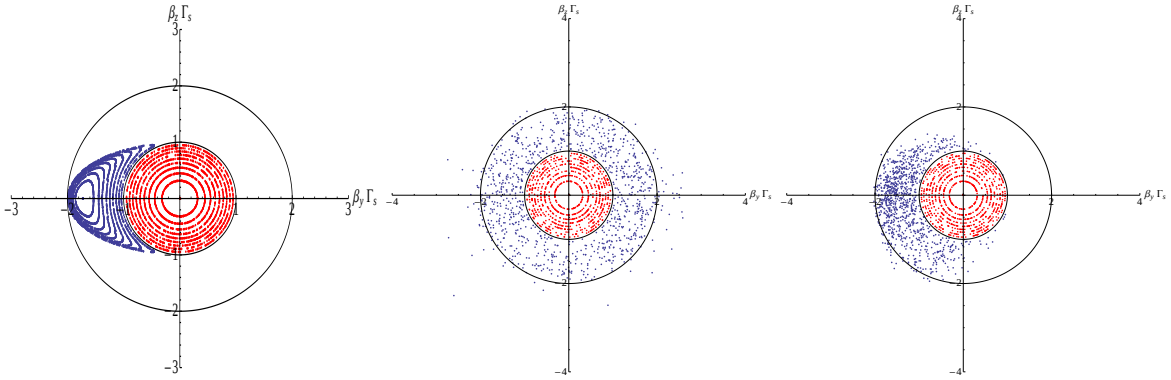

(a) $\vec{B}_0$: locked phase space configuration. No Fermi cycles.

(b) $\delta\vec{B} + \vec{B}_0$, $\rho' \sim 1$, unlocked configuration

(c) $\delta\vec{B} + \vec{B}_0$, $\rho \gg 1$

Fig. 3: Three plots of upstream velocity space in shock front plane: $\beta_y\Gamma_S$ vs $\beta_z\Gamma_S$. Shock front propagates along x direction. Red dots: entry from downstream. Blue dots: escape to downstream.

These results are in qualitative agreement with direct simulations of Niemiec et al. (2006) of particle acceleration including small-scale intense magnetic fields in the downstream region. When B_0 and large-scale compressed field are present these authors observed acceleration cut-off.

Diffusive acceleration is not effective enought to span several orders of magnitude in energy. Small-scale turbulence is effective at the beginning of the process. But if the extenal medium is magnetised the acceleration process is quenched rapidly.

5 Conclusion

In this proceeding a study of particle transport in small-scale intense magnetic turbulence was presented. We found that:

- When particle energy is high (e.g. $\rho >> 1$), B_0 is kinematically important, and the particle transport is anisotropic, even if $\delta B^2 >> B_0^2$, as illustrated in Fig. 1. The diffusion coefficients (Eq.3.1) have been derived with a theory that is exact in the limit of a short correlation time $\tau_c << \tau_s$.
- Diffusive shock acceleration in small-scale turbulence appears to be effective only when $1 < \rho < \sqrt{\delta B^2/B_0^2}$.

Conclusions about acceleration performances might be modified if coherence length of the turbulence grows with time, additionnal source of magnetic turbulence on large scale is present in downstream region.

References

Achterberg, A., Gallant, Y. A., Kirk, J. G., & Guthmann A. W. 2001, MNRAS 328, 393

Casse, F., Lemoine, M., & Pelletier, G. 2002, Phys. Rev. D, 65, 023002

Lemoine, M., Pelletier, G., & Revenu, B. 2006, ApJL, 645, 129

Li, Z., & Waxman, E. 2006, ApJ, 651, 328

Niemiec, J., Ostrowski, M., Pohl, M. 2006, ApJ, 650, 1020

Plotnikov, I., Pelletier, G., Lemoine, M., 2011, A&A, 532, 68

Sironi, L., & Spitkovsky, A. 2011, ApJ, 726, 75